Comparison for Various Kinds of Hamiltonian in Graphene Nanoribbon Quantum Transport Calculation

Jikun Ding, Qiming Shao, Jinyu Zhang, and Zhiping Yu
Institute of Microelectronics, Tsinghua University, Beijing 100084, China
Tel: +86-10-6277-1283, Fax: +86-10-6279-5104, Email: zhangjinyu@tsinghua.edu.cn

Abstract—**The band structure and transport of an armchair and the zigzag graphene nanoribbon (GNR) are calculated using different types of Hamiltonians, including density functional-based tight binding (DFTB), extended Hückel theory (EHT), tight binding (TB), and density functional theory (DFT). Only the p_z orbit is used for the carbon atom in the TB Hamiltonian (p_z-TB). The other four orbits are used for the carbon atoms in the DFTB and EHT Hamiltonians. The transport calculation is performed using non-equilibrium Green's function (NEGF). The results show that all Hamiltonians have consistent band structures and I-V characteristics. Although p_z-TB has low accuracy in describing the defects on GNR, it can still provide qualitatively correct band structures and I-V curves.**

Keywords-Graphene nanoribbon; DFTB; EHT; p_z-TB; DFT; NEGF; defects

I. INTRODUCTION

Various Hamiltonians are used in band structure and quantum transport calculations to evaluate carbon-based device performance. Density functional theory (DFT) calculation [1][2] is considered as the most fundamental and accurate method among the Hamiltonians. However, due to its huge computational cost, it is usually applied in small system. Density functional-based tight binding (DFTB) [3] and extended Hückel theory (EHT) [4] Hamiltonians are two candidates for larger systems with the disadvantage of accuracy loss. The p_z orbit is used for the carbon atom in the TB Hamiltonian (p_z-TB) is widely used in transport calculations because of its lower computational cost compared with the other three methods. DFT calculations [5] have recently shown that asymmetric zigzag grapheme nanoribbon (ZGNR) exhibits conventional metallic conductance under bias, whereas symmetric ZGNR exhibits semiconductor-like conductance (called the odd-even effect in this study). The reason for this is that the transmission through the system depends on whether π electrons can hop to the π^* state or not (π and π^* refer to the two bands near the Fermi level in the E-k diagram). For the symmetric ZGNR, the hopping integral is zero because of σ parity limitation, whereas such constraint is not observed for the asymmetric ZGNR. In graphene antidote lattices (GALs), electronic localized states have been demonstrated [6] to be equal to $|n\alpha - n\beta|$ ($n\alpha$ and $n\beta$ are the number of removed α and β type atoms in GALs) of the supercell. Whether EHT, DFTB and p_z-TB can reproduce such effects remains unclear. Although a number of studies on band structure calculations have been conducted using various types of Hamiltonians, only few studies have compared their transport properties. In this study, the band structures of GNR and the transport properties of a two-terminal GNR device are calculated to test the consistency of DFT, DFTB, EHT, and p_z-TB.

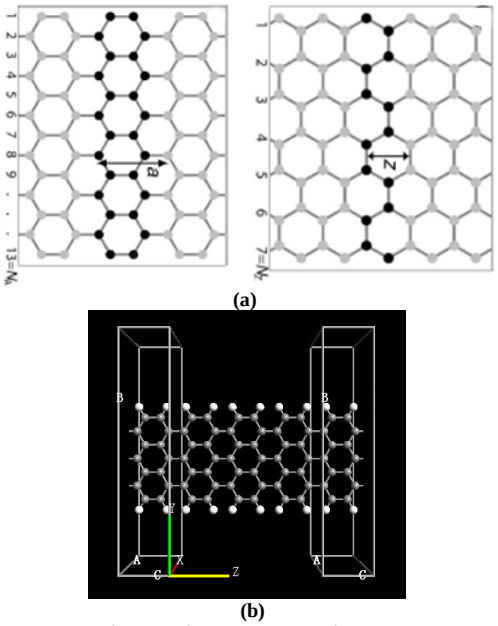

Fig. 1 (a) Symbolic definition of the parameters of AGNR and ZGNRs. The black balls represent the unit cells and a and z represent the unit cell width of AGNR and ZGNR, respectively. (b) Two-terminal GNR-based device structure. Atoms in the cuboid are electrodes.

II. METHODOLOGY

Following the standard convention [6], as shown in Fig. 1(a), the width of the armchair GNR (AGNR) is defined as the number

 ISBN 978-0-615-71756-2

of dimer lines along the vertical direction (N_a) and the width of the ZGNR is defined as the number of zigzag chains along the horizontal direction (N_z). AGNR (ZGNR) with width N_a (N_z) is labeled as N_a-AGNR (N_z-ZGNR).

The Atomistix ToolKit (ATK) was used to perform GNR device band structure and transport calculations by using DFT Hamiltonian. Coding was performed to implement device simulation by using p_z-TB, DFTB, and EHT combined with NEGF. Fig. 1(b) shows the schematic diagram of the simulated

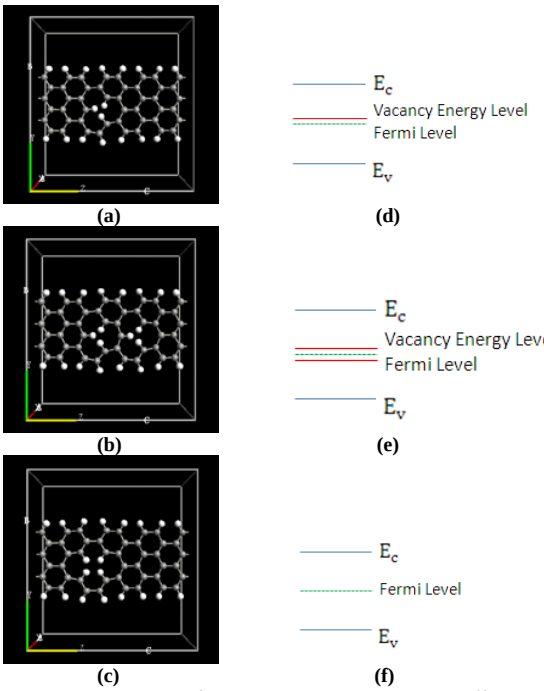

Fig. 2 Schematics diagram of the simulated structure with different vacancy configurations. The grey and white balls represent carbon and hydrogen atoms, respectively. (a), (b), and (c) represent the configurations of V_a, V_{aa}, and V_{ab}, respectively. (d), (e), and (f) schematically show the corresponding band structures.

structure. After DFT geometry relaxation, the distances of C-C and C-H were 1.422 and 1.101 Å, respectively, which were consistent with the results of previous calculations [7]. The edge carbon distance is relaxed at 3.5% (the hopping integral increased by 12%) to describe GNR edge relaxation in the p_z-TB model [7]. The Hamiltonian constructions of EHT and DFTB consisted of four orbits for the carbon atom and a single orbit for the hydrogen atom. On the other hand, in the p_z-TB Hamiltonian, only the p_z orbit was used for the carbon atom and the orbit of the hydrogen atom was ignored. The parameters of the DFTB and EHT Hamiltonians were obtained from refs. [8] and [9], respectively. The hopping integral between C-C in p_z-TB model was 2.7 eV. The NEGF implementation followed the standard procedure [11] to be solved with Poisson's equation self-consistently. Fig. 7 shows the flowchart and Table 3 lists the main equations that were used within the NEGF formulism.

In addition to the perfect AGNR, three configurations of AGNR with vacancy defects were used in the band structure and transport calculations. As can be seen in Figs. 2(a)–2(c), V_a, V_{aa}, and V_{ab} were used to denote the removal of one C atom, two identical type C atoms, and two different types of C atoms, respectively. All the configurations were optimized using ATK with force tolerance of 0.05 eV/Å. According to Ref. [6], the number of defects level for V_a, V_{aa}, and V_{ab} should be 1, 2 and 0, respectively, as shown in Figs. 2(d)–2(f).

III. Results and Discussions

Fig. 5 shows four bands near the Fermi level and I-V curves of 7-, 8-, and 9-AGNR. Fig. 3 shows the band structures and I-V curves of 7- and 8-ZGNR. The results show that the four Hamiltonians can provide similar band structures and comparative I-V curves. The results can be verified by the fact that the bias where the current rises is nearly equal to the energy band gap of the corresponding configuration, matching the proposed manifestation. The odd-even effect can be reproduced using p_z-TB, as shown in Fig. 4. This result is consistent with the first principle calculation [5]. DFTB and EHT also possess the odd-even effect (the results are not shown here).

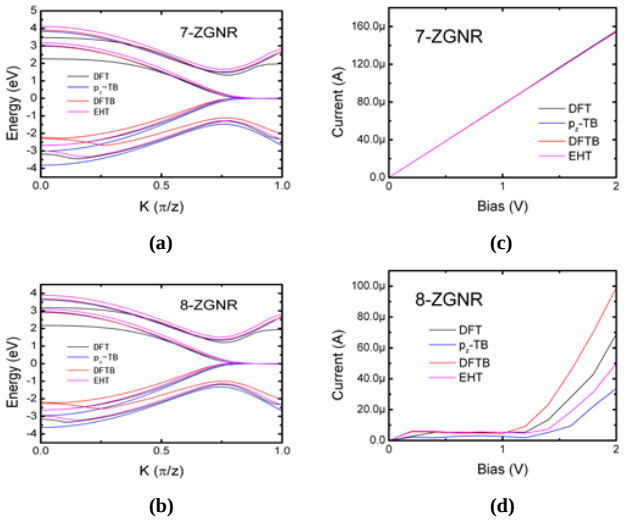

Fig. 3 Comparisons of the electronic and transport properties of ZGNR by using four Hamiltonians. (a) and (b) represent the band structure of 7-ZGNR and 8-ZGNR, respectively. (c) and (d) represent the corresponding I-V curves.

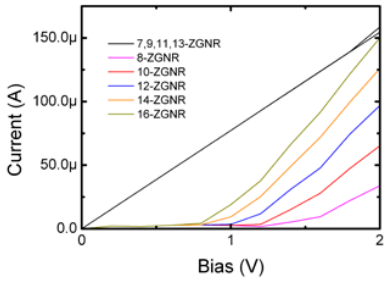

Fig. 4 Demonstration of the odd-even effect by using p_z-TB.

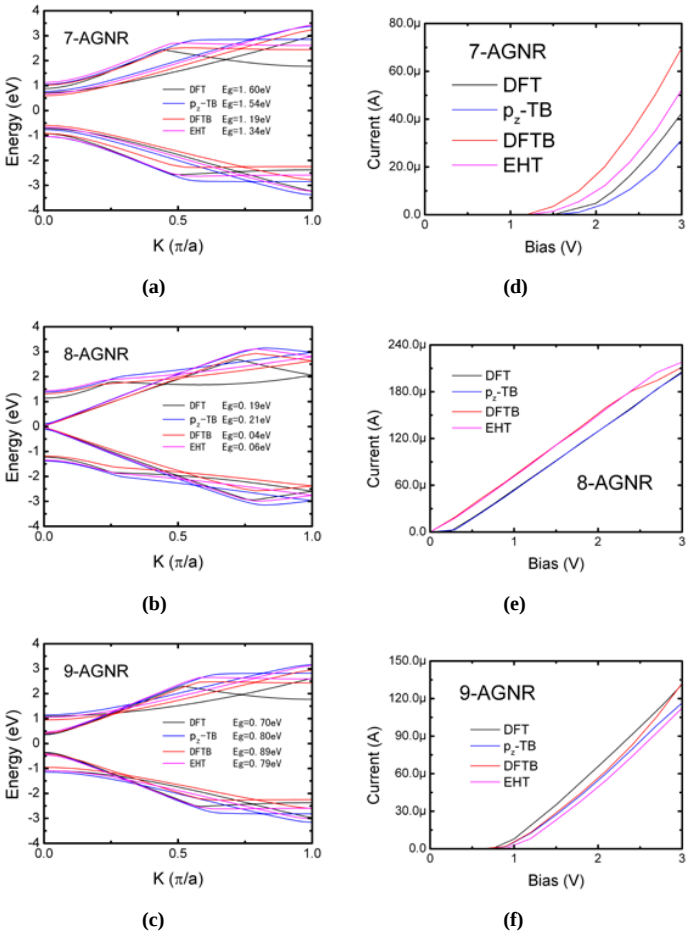

Fig. 5 Comparisons of the electronic and transport properties of AGNRs by using four Hamiltonians. (a)–(c) are band structure of 7-AGNR, 8-AGNR and 9-AGNR, respectively. (d)–(f) are corresponding I-V curves.

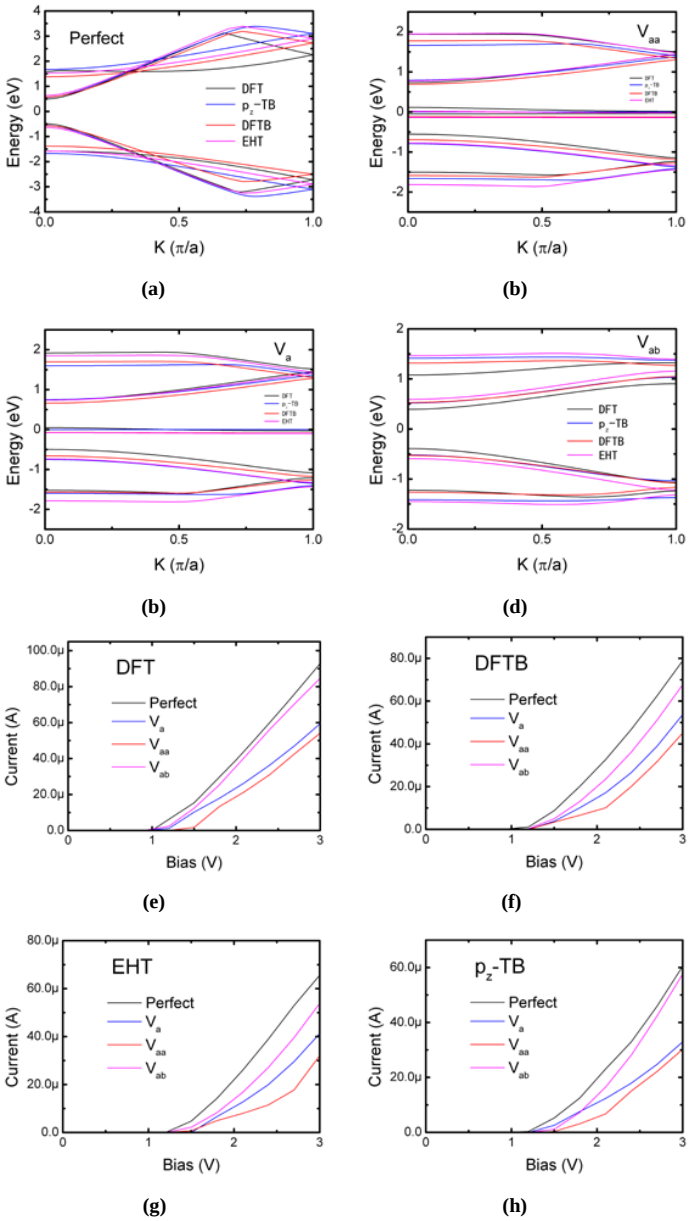

Fig. 6 Comparisons of the electronic and transport properties of 6-AGNR with defects by using four Hamiltonians. (a)–(d) are the band structures of perfect, V_{aa}, V_a, and V_{ab}, respectively. (e)–(h) are the corresponding I-V curves.

In this study, the band structure of GNR with vacancy defects and the transport properties of related GNR devices were investigated to further verify the consistency of the four Hamiltonians. Figs. 6(a)–6(d) show the band structures with different defects configurations by using four kinds of Hamiltonians. The defects in energy levels for all the Hamiltonians were consistent with the rule mentioned in Ref. [6]. Figs. 6(e)–6(h) provide the corresponding I-V curves. The results show that the current does not simply increase or decrease with increasing vacancy number, but is rather closely related to the type and number of removed C atoms. Tables 1 and 2 summarize the energy band gap and current for different defect configurations by using four Hamiltonians. The discrepancies among the currents of DFT, DFTB, and EHT Hamiltonians can be attributed to the energy band gap

difference, where the smaller energy band gap usually leads to a larger current. However, such result is not true for p_z-TB, such as in the V_{aa} configuration. Suppose that the use of the p_z orbit alone may be insufficiently accurate to describe defect configurations. The hopping integral within the p_z-TB model can be estimated to change around the vacancy spot because of the relaxation that accounts for the variation in chemical environment compared to the perfect lattice. The calculated 2.7 eV parameter within the p_z-TB model cannot precisely describe the situation under this circumstance. However, the results of band structure and transport properties are qualitatively correct, and thus, p_z-TB can still be useful for GNR device simulation.

IV. CONCLUSION

Four kinds of Hamiltonians, including DFTB, p_z-TB, EHT, and DFT were used to calculate the band structure and transport properties of GNR devices. The DFTB, p_z-TB, and EHT models were shown capable of revealing physics in refs. [5] and [6] with less computational burden compared with the DFT model. The results of the four Hamiltonians were consistent for perfect GNR. For the GNR with vacancy defects, p_z-TB exhibited lower accuracy than the other three Hamiltonians, but it was able to provide qualitatively correct band structure and transport properties with the lowest computational cost. Moreover, the impact of vacancies in GNR device was proposed to be closely related to the type of the atoms removed.

ACKNOWLEDGMENT

This work was supported by the Important National Science and Technology Specific Projects (Grant No. 2011ZX02707), National Major Science Plans (Grant No. 2011CBA00604 and 2011CB933004), National Science Foundation (Grant No. 60876073) and Tsinghua National Laboratory for Information Science and Technology. The authors would like to thank the other members of Prof. Zhiping Yu's group in the Institute of Microelectronics, Tsinghua University, for the helpful discussions. We would also like thank Hao Nan for his patience in instructing NEGF formulism. Hao Nan is currently a doctorate student in Stanford University.

REFERENCE

[1] P. Hohenberg and W. Kohn, Phys. Rev. 136, B864 (1964).
[2] S. F. Sousa, J. Phys. Chem. A 111, 10439 (2007).
[3] P. Koskinen *et al.*, Computational Material Science, 47, 237 (2009).
[4] R. Hoffmann, J. Chem. Phys. 39, 1297(1963).
[5] Z. Li, *et al.*, Phys. Rev. Lett. 100, 206802 (2008).
[6] F. Ouyang, *et al.*, J. Phys. Chem. C 114, 15578(2010).
[7] Y. Hancock, *et al.*, Phys. Rev. B 81, 245402 (2010).
[8] Y. Son , *et al.*, Phys. Rev. Lett. 97, 216803 (2006).
[9] Density Functional based tight binding. http://www.dftb.org/
[10] Cerda J. EHT parameters for some elements and compounds. http://www.icmm.csic.es/jcerda/
[11] S. Datta, Superlattices and Microstructures, Vol. 28, No. 4, 2000.

Table 1 Comparisons energy band gaps for different vacancy configurations using four kinds of Hamiltonians. Unit is eV.

Hamiltonian	Perfect	V_a	V_{aa}	V_{ab}
DFT	0.98	1.23	1.29	0.78
DFTB	1.13	1.32	1.39	1.06
EHT	1.25	1.47	1.56	1.18
p_z-TB	1.12	1.50	1.58	1.04

Table 2 Comparisons of the electric currents of different vacancy configurations by using four kinds of Hamiltonians. The currents (units in μA) are measured at a bias of 2.4 V.

Hamiltonian	Perfect	V_a	V_{aa}	V_{ab}
DFT	60.0	36.1	31.0	56.2
DFTB	46.8	26.6	20.0	36.1
EHT	38.9	19.9	11.5	27.1
p_z-TB	32.9	17.9	15.0	28.1

$$\Gamma_S = i[\Sigma_S - \Sigma_S^\dagger] \quad \Gamma_D = i[\Sigma_D - \Sigma_D^\dagger] \qquad \text{(Eq. 1)}$$

$$G(E) = [EI - H - \Sigma_S - \Sigma_D]^{-1} \qquad \text{(Eq. 2)}$$

$$A(E) = i[G - G^\dagger] = G\Gamma_S G^\dagger + G\Gamma_D G^\dagger \qquad \text{(Eq. 3)}$$

$$G^n(E) = G\Gamma_S G^\dagger f_S + G\Gamma_D G^\dagger f_D \qquad \text{(Eq. 4)}$$

$$I = \int dE Trace[\Gamma_S G \Gamma_D G^\dagger][f_S(E) - f_D(E)] \qquad \text{(Eq. 5)}$$

Table 3 Main equations used in NEGF calculations. Subscript S and D stand for the source and drain respectively within simulation region. Eq. 1 is used to calculate the broadening matrixes due to source and drain. Σ is the self-energy matrix. Eq. 2 is the equation for Green's function. I is identity matrix and H is Hamiltonian of the device. Eq. 3 is used to calculate the spectrum function and Eq. 4 is for the correlation function whose diagonal elements are the local electron density. f is Fermi-Dirac function. Eq. 5 is the net current through the simulated device.

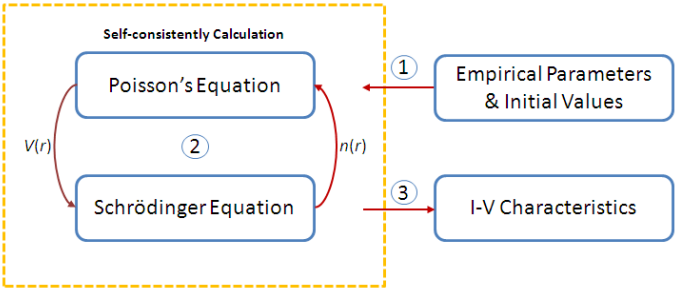

Fig. 7 Flow chart for the NEGF and Poisson's Equation self-consistent calculation.